



Laser cooling of the Yb³⁺-doped LuLiF₄ single crystal for optical refrigeration

Biao Zhong^{a,b}, Yongqing Lei^a, Hao Luo^a, Yanling Shi^b, Tao Yang^{a,c,*}, Jianping Yin^{a,**}

^a State Key Laboratory of Precision Spectroscopy, East China Normal University, Shanghai, 200062, PR China

^b School of Information Science and Technology, East China Normal University, Shanghai, 200062, PR China

^c Collaborative Innovation Center of Extreme Optics, Shanxi University, Taiyuan, Shanxi, 030006, PR China

ABSTRACT

A vibration-free, optical cooling refrigerator may imply revolutionary applications in different fields, therefore it is vital to explore new materials suitable for laser cooling below the cryogenic temperature. Here we demonstrate that the Yb³⁺-doped LuLiF₄ crystal is a promising material that could reach the cryogenic temperature limit (123 K) or even lower. With the doping concentration of 7.5%, the Yb³⁺-doped LuLiF₄ crystal can be optically cooled down from the room temperature to 141.8 K in a double-pass setup. Provided with better purity and multiple-pass of laser cooling in the crystal, the temperature limit can even reach as low as 89 K for the 7.5% Yb³⁺-doped LuLiF₄ crystal, thus making it a competitive candidate for laser cooling below the cryogenic temperature.

1. Introduction

Solid state refrigerators have attracted substantial attentions in the fields of biology, military technology, space exploration, precise measurement, and material sciences [1–10]. Laser-powered cryocoolers can benefit to the application of ultra-stable lasers and interferometers, which are extremely sensitive to vibration [4,5]. Compact cold-fingers with no moving parts in the optical refrigerator can play an important role in devices such as the infrared cameras/detectors and Gamma-ray spectrometers [2,11]. Since the first experimental realization of refrigeration via anti-Stokes fluorescence in Yb³⁺-doped ZBLANP fluoride glass [2], optical cooling has been developed in different glasses such as Yb³⁺ doped in ZBLAN(P) [2,11–13], CNBZn [14], BIG [12], ABCYS [15], Tm³⁺ doped in ZBLAN [16], and Er³⁺ doped in CNBZn [17]. Considering that the rare-earth ion can generally have relatively smaller ground-state energy splitting and higher doping concentration in the crystal than in the glass [18], efforts have been made to explore new crystals that are practical for solid state optical refrigerators [19], such as Yb³⁺ doped in KYF₄ [20], KGd(WO₄)₂ [21], KY(WO₄)₂ [21], YAG [22], KPb₂Cl₅ [12], BaY₂F₈ [23], YLiF₄ [24–26] and LuLiF₄ [27,28] Tm³⁺ doped in BaYF₄ [29], Er³⁺ doped in KPb₂Cl₅ [17] as well as Ho³⁺ doped in YLiF₄ [30]. Recently, the Sheik-Bahae group cooled the Yb³⁺/Tm³⁺ co-doped YLiF₄ crystal of ultra-high purity from the room temperature to 87 K by laser [31,32]. Semiconductors or lead halide perovskites also find their potentials in laser cooled refrigerators. The Xiong group cooled the

cadmium sulfide nanoribbons in vacuum, followed by cooling the exfoliated 2D perovskite crystals in the room-temperature environment [10,33]. The Kashyap group studied laser cooling of Yb³⁺-doped yttrium aluminum garnet exposed to air [34]. Optical refrigeration of Yb³⁺-doped YLiF₄ nanocrystal and Yb³⁺-doped β-NaYF₄ nanowire immersed in physiological media has been reported by the Pauzauskis group [6].

Based on our previous experimental work, we predicted that Yb³⁺-doped LuLiF₄ single crystal has attractive optical refrigeration properties [27,28], and we would like to further investigate the cooling potential of the crystal after reducing its impurity, increasing Yb³⁺-doped concentration as well as upgrading the experimental setup such as the home-made high-power fiber laser and the utilization of the vacuum system. Here, we report that an Yb³⁺-doped LuLiF₄ crystal grown by the Czochralski method [24] can be optically cooled using a CW fiber laser (1020 nm) with power up to 33 W. The 7.5% Yb³⁺-doped LuLiF₄ crystal was cooled from the room temperature to 152.4 K and 141.8 K by singly and doubly passing the crystal respectively, indicating better cooling potential than the crystal of 5% doping concentration which reached 177.2 K in a single-pass setup. Provided with better purity and multiple-pass of laser cooling in the crystal, the temperature limit can reach as low as 89 K for the 7.5% Yb³⁺-doped LuLiF₄ crystal, thus making it a promising candidate that can reach the liquid nitrogen point (77 K).

Laser cooling of solids is based on Anti-Stokes fluorescence processes

* Corresponding author. State Key Laboratory of Precision Spectroscopy, East China Normal University, Shanghai, 200062, PR China.

** Corresponding author.

E-mail addresses: tyang@lps.ecnu.edu.cn (T. Yang), jpyin@phy.ecnu.edu.cn (J. Yin).

which can be illustrated in a multiple energy level system (Fig. 1a inset) [1]. According to Sheik-Bahae/Epstein theory [3], the cooling efficiency η_c can be express as

$$\eta_c(\lambda_l, T) = 1 - \eta_{\text{ext}} \eta_{\text{abs}} \lambda_l / \lambda_f \quad (1)$$

where λ_l represents the wavelength of the pump laser, T represents the sample temperature, and λ_f represents the average wavelength of the fluorescence that includes the effect of fluorescence re-absorption. The external quantum efficiency η_{ext} can be defined as $\eta_{\text{ext}} = \eta_e W_{\text{rad}} / (\eta_e W_{\text{rad}} + W_{\text{nrad}})$, where η_e is the fluorescence extraction efficiency, with W_{rad} and W_{nrad} representing the radiative and non-radiative recombination rates, respectively. The absorption efficiency η_{abs} is given by the ratio of $\alpha_r / (\alpha_b + \alpha_r)$, where α_r represents the resonant absorption coefficient of the doped rare-earth ion, and α_b is the background absorption coefficient originating from unwanted transitions of metal impurities. A low parasitic absorption (re-absorption of emitted fluorescence photons by the host including metal impurities) and a very high η_{ext} of the host material are essential to the realization of net optical cooling of solids. Also, according to the laser cooling process analyzed by Hehlen, the cooling efficiency depends crucially on the ground-state splitting of the doped rare-earth ion in the host [18]. With small ground-state energy splitting, the initial state of the anti-Stokes pumping transition can be easily populated in the host, which helps to maintain the closed cycling condition as well as the cooling efficiency of the optical refrigerator. Additionally, a smaller ground-state splitting of rare-earth ion doped in the host can lead to smaller inhomogeneous broadening and higher rare-earth ion concentration, both giving a larger peak absorption cross section of the cooling transition [35].

2. Experimental details

Our crystals were grown from LiF, LuF₃ and YbF₃ of high purity with the growth direction being (110). The LiF worked as the small optical crystal, while LuF₃ was made in a way that the Lu₂O₃ was melted in a Pt hydrofluorinator and converted to the fluoride using HF gas. YbF₃ was obtained in a similar way. The fluoride components in a stoichiometric ratio were mixed and loaded in a vitreous carbon crucible and placed in the growth furnace filled with nitrogen of 99.999%. Fig. 1b shows the schematic of the LuLiF₄ crystal. Yb³⁺ ions substitutionally enter the Lu³⁺ sites with point symmetry S4 and coordination number 8, and the charge compensation as well as distortions of the unit cell can be negligible due to the minor difference in the ionic radii between Yb³⁺ and Lu³⁺ [36]. The maximum phonon energy of LuLiF₄ crystal is about ~450 cm⁻¹ [18, 36]. The polarization absorption spectrum of the 5% Yb³⁺-doped LuLiF₄ crystal is presented in Fig. 1a, with the red solid line corresponding to the case of the E//c orientation. The absorption coefficient of the E//c

orientation is larger than that of E//a in the long wavelength range. The blue line represents the unpolarized fluorescence spectrum of the 5% Yb³⁺-doped LuLiF₄ crystal. The average fluorescence wavelength is calculated to be about 998.3 nm at room temperature according to the equation $\lambda_f = \int \lambda S(\lambda, T) d\lambda / \int S(\lambda, T) d\lambda$, where $S(\lambda, T)$ is the temperature-dependent emission spectrum of the crystal.

Prior to measuring the temperature of the crystal during the experiment, we first obtained the temperature calibration curve using the differential luminescence thermometry (DLT) [25]. In Fig. 2a, the Yb³⁺-doped LuLiF₄ crystal, whose surfaces were highly polished with dimensions of 2 × 2 × 5 mm³, was placed inside a vacuum chamber (1 × 10⁻⁴ Pa) and irradiated by a fiber laser tunable from 1010 nm to 1080 nm (The output power of the laser can be greater than 30 W when the wavelength of the laser in the range 1018 nm–1080 nm, and decrease dramatically to a few watts from 1018 nm till 1010 nm). The front and rear surfaces of the crystal were cut at Brewster angles, and the maximum incident laser power onto the crystal was measured to be 33 W at 1020 nm. The crystal was placed on two fibers of 100 μm in diameter and further supported by two pairs of steel rods. The fluorescence of the crystal excited by the pump laser was collected by a fiber of 600 μm in diameter and transported to a spectrometer. The temperature of the crystal was measured by non-contact DLT, and after the illumination of about 15 min, the crystal was stabilized in temperature, indicating that the cooling power of the crystal balances with the heat load from the environment. The convective heat load from the residual gas in the high vacuum and the contact with the fibers can be ignored.

3. Results and discussions

The radiative heat load mainly comes from the blackbody radiation of the environment. Therefore, one has [35].

$$P_{\text{pump}}(1 - \exp[-\alpha l])\eta_c = \sigma_B A_s \varepsilon_s (T_e^4 - T^4) / (1 + \chi) \quad (2)$$

Here, P_{pump} is the power of the pump laser, α and l are the absorption coefficient and the length of the crystal, σ_B is the Stefan-Boltzmann constant, T_e and T are the temperatures of the environment and the crystal respectively. In addition $\chi = (1 - \varepsilon_e)\varepsilon_s A_s / \varepsilon_e A_e$, with A and ε being the corresponding surface and the thermal emissivity. The subscripts s and e denote the sample and the environment (vacuum chamber), respectively. In order to cool the Yb³⁺-doped crystal down below 100 K, the condition of $\eta_{\text{ext}}\eta_{\text{abs}} > 0.99$ has to be satisfied [25]. Here, η_{abs} is determined by the ratio of α_b/α_r , which can be improved by either reducing the impurities or increasing the doping concentration. Fig. 2b shows the temperatures of the crystal as a function of P_{pump} at two different wavelengths, with the solid lines fitting the data best according to equations (1) and (2), leading to $\eta_{\text{ext}} = 0.994$ and $\alpha_b = 4.5 \times 10^{-4}$

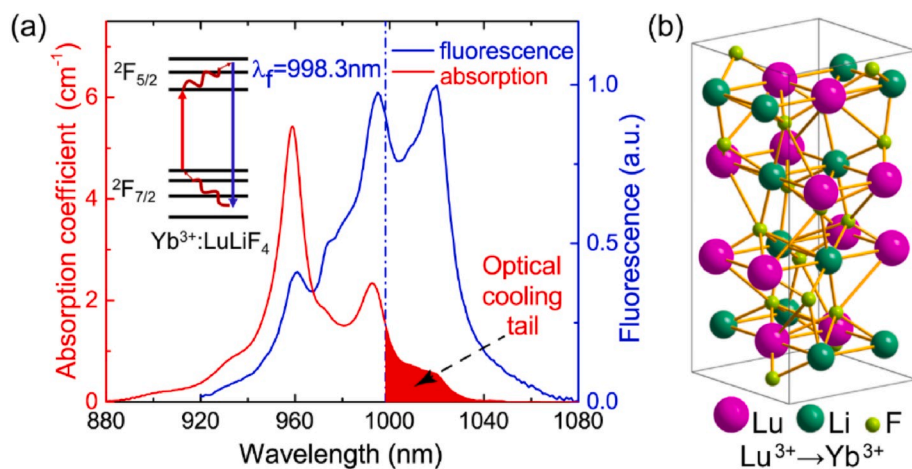


Fig. 1. (a) The absorption and fluorescence spectra of the 5% Yb³⁺-doped LuLiF₄, with the inset of the multiple energy level system of the Yb³⁺. The blue vertical dotted line represents the average fluorescence wavelength at around 998.3 nm at room temperature. The red shaded area, called the optical cooling tail, represents the absorption spectrum for photon energies below the mean fluorescence energy. (b) The schematic structure of the Yb³⁺-doped LuLiF₄ crystal. (For interpretation of the references to colour in this figure legend, the reader is referred to the Web version of this article.)

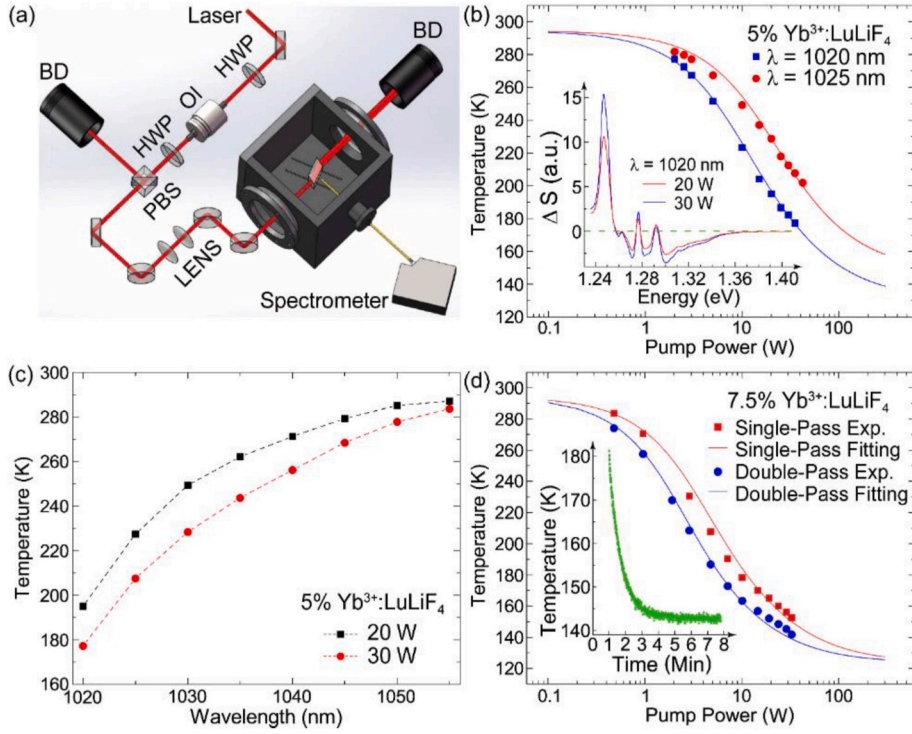


Fig. 2. (a). Experimental schematic of the optical cooling setup. HWP: Half Wavelength Plate; OI: Optical Isolator; PBS: Polarization Beam Splitter; LENS: $f_1 = 50$ mm, $f_2 = 100$ mm; BD: Beam Dump. (b). Temperature dependence of the 5% Yb³⁺-doped LuLiF₄ crystal on the P_{pump} ; the inset shows the differential luminescence spectra ΔS of the laser-cooled crystal with respect to that at 294.5 K for $P_{\text{pump}} = 20$ W and 30 W. (c). Temperature dependence on the pump laser wavelength of the 5% Yb³⁺-doped LuLiF₄ crystal. (d). Temperature dependence of the 7.5% Yb³⁺-doped LuLiF₄ crystal at 1020 nm on the P_{pump} in the single-pass and double-pass setup respectively, with the inset indicating how the temperature varies with time in the double-pass configuration.

cm^{-1} . The overall cooling effect performs better at the wavelength of 1020 nm, which indicates the resonant absorption and matches the value of the ridge in the optical cooling tail of Fig. 1a. For the 5% Yb³⁺-doped LuLiF₄ crystal, we reached the temperature of 177.2 K when P_{pump} was 33 W at 1020 nm. The crystal was also studied as a function of the laser wavelength with the fixed P_{pump} (Fig. 2c), showing that the cooling effect exhibits better performance for the crystal with higher incident laser power. We studied the laser cooling of the 7.5% Yb³⁺-doped LuLiF₄ crystal as well, and obtained the dependence of the temperature on the P_{pump} at the fixed wavelength of 1020 nm, which was further fitted based on that $\eta_{\text{ext}} = 0.998$ and $\alpha_b = 7.5 \times 10^{-4} \text{ cm}^{-1}$ (Fig. 2d). It is well established that among the transition metal ions, Fe²⁺ plays the major role in the background absorption than the others [37]. Utilizing the GDMS methods, we noticed that the Fe²⁺ concentration in the 5% and 7.5% Yb³⁺-doped LuLiF₄ crystals are about 0.5 ppm and 1 ppm, respectively. Since the impurity metal ion concentration is linearly dependent of the natural logarithm of α_b [37], it is therefore to conclude that the α_b is larger in the 7.5% Yb³⁺-doped LuLiF₄ crystal than that in the 5% Yb³⁺-doped crystal, which agrees with our fitting results that α_b is smaller in the 5% doping crystal as well. However, the absorption efficiency η_{abs} is eventually determined by the ratio of α_b/α_r , where α_r in 7.5% Yb³⁺-doped LuLiF₄ crystal is 1.5 times of that in the 5% Yb³⁺-doped crystal. Considering the fitting values of α_b and the ratio of α_r between the two crystals, we figured out that η_{abs} for the 7.5% Yb³⁺-doped LuLiF₄ is larger and should push the temperature down to a lower limit. The cooling temperatures of 152.4 K and 141.8 K at the P_{pump} of 33 W were obtained respectively in the single-pass and double-pass setups of the 7.5% Yb³⁺-doped LuLiF₄ crystal, with the absorption powers of about 2.2 W and 3.3 W as well as the heat load powers of 17.1 mW and 17.4 mW, all of which lead to the respective cooling efficiency of about 0.8% and 0.5% according to equation (1). An extrapolation of this fitting curve indicates that the lowest temperature of this crystal can approach 121 K, which is already below the cryogenic temperature of 123 K defined by NIST (National Institute of Standards and Technology).

The crystal can be further cooled down by reducing the heat load of the blackbody radiation from the surrounding environment, and

improvement towards increasing the value of χ can effectively suppress the emissivity of the chamber surface around the crystal [35]. For instance, the Maxorb foil stuck onto the chamber wall can reduce the blackbody heat load on the crystal by a factor of six [25]. Based on our experimental results, the cooling window of the 5% Yb³⁺-doped LuLiF₄ crystal ($\alpha_b = 4.5 \times 10^{-4} \text{ cm}^{-1}$) is plotted in Fig. 3a, and its minimum achievable temperature is estimated to be about 112 K. The cooling window of 7.5% Yb³⁺-doped LuLiF₄ crystals was calculated based on $\alpha_b = 1.0 \times 10^{-4} \text{ cm}^{-1}$, which is assumed to be the same as that in the 10% Yb³⁺-doped YLiF₄ crystal [26]. As a result, the crystal can reach a temperature as low as 89 K as shown in Fig. 3b, indicating that our 7.5% Yb³⁺-doped LuLiF₄ crystal has the same cooling potential as the 10% Yb³⁺-doped YLiF₄ crystal. It is also noticeable that the best cooling point can be obtained at around 1020 nm, which agrees nicely with the results we had. Increasing the Yb³⁺-doped ion concentration can increase the absorption of P_{pump} , however, cooling the crystal of the critical concentration $N_0 = 7.47 \times 10^{21} \text{ cm}^{-3}$ will be destructive due to the cooperative effects [38,39]. Fortunately, such an effect can be much alleviated in the 7.5% Yb³⁺-doped LuLiF₄ since the Yb³⁺ ion concentration is about $1.08 \times 10^{21} \text{ cm}^{-3}$.

After the examination of the cooling performance of the 5% and 7.5% Yb³⁺-doped LuLiF₄ crystals, we propose that a possible cooling candidate may possess the properties such as high η_{ext} which requires low non-radiative recombination and low refraction index, high absorption efficiency η_{abs} which demands large rare-earth ion doping concentration, and low background absorption which requires ultra-high purity. Compared to the glass of the amorphous structure, the crystalline structure of the crystal contributes less to the inhomogeneous broadening of the ion absorption and can increase the peak absorption cross section as well [19]. Besides, the crystal can accept even larger ion doping concentration than the glass [35]. In addition, the small crystal-field induced splitting of the doping rare-earth ion offers more thermal population of the initial state of the pumped transition. These are important for the laser cooling of the crystal, especially at low temperatures when the population probability of the initial state of the pump transition becomes very small. Finally, the detrimental impurities present in the starting materials always remain inside the glass.

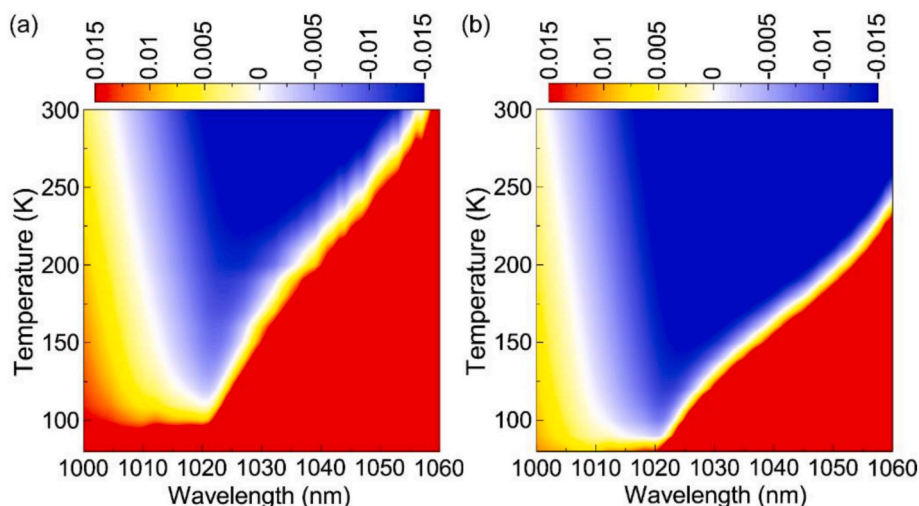


Fig. 3. The cooling windows of the 5% (a) and 7.5% (b) Yb^{3+} -doped LuLiF_4 crystals. The cooling window describes the dependence of the cooling efficiency on both of the crystal temperature and the pump laser wavelength. The blue regions denote cooling, while the red regions represent heating. (For interpretation of the references to colour in this figure legend, the reader is referred to the Web version of this article.)

However, they can be excluded from the crystal during the crystallization process [40]. Therefore, the crystal has more cooling potential than the glass. For instance, the best cooling record of the fluoride glass (Yb^{3+} -doped ZBLANP) was reported to be about 208 K with its minimum achievable temperature predicted to be about 190 K, comparing with the experimental record of 141.8 K and the minimum achievable temperature of 89 K for the Yb^{3+} -doped LuLiF_4 crystal, and the best cooling record of 87 K [32,41] and the minimum achievable temperature of 89 K for the Yb^{3+} -doped YLiF_4 crystal, respectively [26].

4. Conclusion

To conclude, we have demonstrated that the Yb^{3+} -doped LuLiF_4 crystal can be optically cooled down to temperatures closed to the cryogenic one. The 5% Yb^{3+} -doped LuLiF_4 crystal was cooled to 177.2 K when being irradiated by a laser of about 33 W at 1020 nm, while the 7.5% Yb^{3+} -doped LuLiF_4 crystal was cooled down to even lower temperatures of 152.4 K and 141.8 K when being exposed to the same laser respectively in a single-pass or double-pass setup. Our simulation of the 5% Yb^{3+} -doped LuLiF_4 crystal with the current purity indicate that its global minimum achievable temperature was 112 K, while for 7.5% Yb^{3+} -doped LuLiF_4 crystal with a purity of $\alpha_b = 1.0 \times 10^{-4} \text{ cm}^{-1}$ this temperature can be further brought down to 89 K. We believe that, improvement on the thermal management, crystal purity, pump laser absorption (such as using the Herriott cell [31]) and Yb^{3+} -doped concentration, should push the cooling temperature of the Yb^{3+} -doped LuLiF_4 crystal down to an even lower limit, thus making it a promising laser cooling crystal that can eventually be used as an all-solid-state cryogenic optical refrigeration medium.

Author statement

B. Z., T. Y., S. Y. L., and J. P. Y. conceived the approach and supervised the work. Experiments were performed by B. Z., Y. Q. L., and H. L. All authors contributed to the discussion and interpretation of the results. The manuscript was prepared by B. Z., and T. Y. with contributions from S. Y. L., and J. P. Y.

Declaration of competing interest

The authors declare that they have no known competing financial interests or personal relationships that could have appeared to influence the work reported in this paper.

Acknowledgements

We thank the funding support from National Natural Science Foundation of China (11604100, 11834003, 61574056, 91536218 and 11874151), the Special Financial Grant from the China Postdoctoral Science Foundation (2016T90346), Shanghai Pujiang Talents Plan (18PJ1403100), the Natural Science Foundation of Shanghai (14ZR1412000 and 18ZR1412700), the Program for Professor of Special Appointment (Eastern Scholar) at Shanghai Institutions of Higher Learning, and the 111 Project (B12024).

Appendix A. Supplementary data

Supplementary data to this article can be found online at <https://doi.org/10.1016/j.jlumin.2020.117472>.

References

- [1] D.V. Seletskiy, R. Epstein, M. Sheik-Bahae, Laser cooling in solids: advances and prospects, *Rep. Prog. Phys.* 79 (2016), 096401.
- [2] R.I. Epstein, M.I. Buchwald, B.C. Edwards, T.R. Gosnell, C.E. Mungan, Observation of laser-induced fluorescent cooling of a solid, *Nature* 377 (1995) 500–503.
- [3] M. Sheik-Bahae, R.I. Epstein, Optical refrigeration, *Nat. Photon.* 1 (2007) 693–699.
- [4] M.P. Hehlen, M. Sheik-Bahae, R.I. Epstein, S.D. Melgaard, D.V. Seletskiy, Materials for optical cryocoolers, *J. Mater. Chem. C* 1 (2013) 7471–7478.
- [5] T. Kessler, C. Hagemann, C. Grebing, T. Legero, U. Sterr, F. Riehle, M.J. Martin, L. Chen, J. Ye, A sub-40-mHz-linewidth laser based on a silicon single-crystal optical cavity, *Nat. Photon.* 6 (2012) 687–692.
- [6] P.B. Roder, B.E. Smith, X. Zhou, M.J. Crane, P.J. Pauzauskie, Laser refrigeration of hydrothermal nanocrystals in physiological media, *Proc. Natl. Acad. Sci. U.S.A.* 112 (2015) 15024–15029.
- [7] X. Zhou, B.E. Smith, P.B. Roder, P.J. Pauzauskie, Laser refrigeration of ytterbium-doped sodium–yttrium–fluoride nanowires, *Adv. Mater.* 28 (2016) 8658–8662.
- [8] J. Gieseler, B. Deutsch, R. Quidant, L. Novotny, Subkelvin parametric feedback cooling of a laser-trapped nanoparticle, *Phys. Rev. Lett.* 109 (2012) 103603.
- [9] J. Zhang, Q. Zhang, X. Wang, L.C. Kwek, Q. Xiong, Resolved-sideband Raman cooling of an optical phonon in semiconductor materials, *Nat. Photon.* 10 (2016) 600–605.
- [10] S.-T. Ha, C. Shen, J. Zhang, Q. Xiong, Laser cooling of organic–inorganic lead halide perovskites, *Nat. Photon.* 10 (2016) 115–121.
- [11] C. Mungan, M. Buchwald, B. Edwards, R. Epstein, T. Gosnell, Laser cooling of a solid by 16 K starting from room temperature, *Phys. Rev. Lett.* 78 (1997) 1030.
- [12] J.R. Fernandez, A. Mendioroz, R. Balda, M. Voda, M. Al-Saleh, A. Garcia-Adeva, J.-L. Adam, J. Lucas, Origin of laser-induced internal cooling of Yb^{3+} -doped systems, *Proc. SPIE* 4645 (2002) 135–147.
- [13] D.V. Seletskiy, M.P. Hasselbeck, M. Sheik-Bahae, Resonant cavity-enhanced absorption for optical refrigeration, *Appl. Phys. Lett.* 96 (2010) 181106.
- [14] J. Fernandez, A. Mendioroz, A. Garcia, R. Balda, J. Adam, Anti-Stokes laser-induced internal cooling of Yb^{3+} -doped glasses, *Phys. Rev. B* 62 (2000) 3213.

- [15] J.V. Guiheen, C.D. Haines, G.H. Sigel, R.I. Epstein, J. Thiede, W.M. Patterson, Yb^{3+} and Tm^{3+} -doped fluoroaluminate classes for anti-Stokes cooling, *Phys. Chem. Glasses-B* 47 (2006) 167–176.
- [16] C. Hoyt, M. Sheik-Bahae, R. Epstein, B. Edwards, J. Anderson, Observation of anti-Stokes fluorescence cooling in thulium-doped glass, *Phys. Rev. Lett.* 85 (2000) 3600.
- [17] J. Fernandez, A.J. Garcia-Adeva, R. Balda, Anti-Stokes laser cooling in bulk erbium-doped materials, *Phys. Rev. Lett.* 97 (2006), 033001.
- [18] M.P. Hehlen, Crystal-field effects in fluoride crystals for optical refrigeration, *Proc. SPIE* 7614 (2010) 761404.
- [19] D.V. Seletskiy, S.D. Melgaard, R.I. Epstein, A. Di Lieto, M. Tonelli, M. Sheik-Bahae, Precise determination of minimum achievable temperature for solid-state optical refrigeration, *J. Lumin.* 133 (2013) 5–9.
- [20] A. Volpi, G. Cittadino, A. Di Lieto, M. Tonelli, Anti-Stokes cooling of Yb-doped KYF_4 single crystals, *J. Lumin.* 203 (2018) 670–675.
- [21] S. Bowman, C. Mungan, New materials for optical cooling, *Appl. Phys. B* 71 (2000) 807–811.
- [22] G. Nemova, R. Kashyap, Laser cooling in Yb^{3+} : YAG, *J. Opt. Soc. Am. B* 31 (2014) 340–348.
- [23] S. Bigotta, D. Parisi, L. Bonelli, A. Toncelli, M. Tonelli, A. Di Lieto, Spectroscopic and laser cooling results on Yb^{3+} -doped $\text{Ba Y}_2\text{F}_8$ single crystal, *J. Appl. Phys.* 100 (2006), 013109.
- [24] S. Bigotta, A. Di Lieto, D. Parisi, A. Toncelli, M. Tonelli, Single fluoride crystals as materials for laser cooling applications, *Proc. SPIE* 6461 (2007) 64610E.
- [25] D.V. Seletskiy, S.D. Melgaard, S. Bigotta, A. Di Lieto, M. Tonelli, M. Sheik-Bahae, Laser cooling of solids to cryogenic temperatures, *Nat. Photon.* 4 (2010) 161–164.
- [26] S.D. Melgaard, A.R. Albrecht, M.P. Hehlen, M. Sheik-Bahae, Solid-state optical refrigeration to sub-100 Kelvin regime, *Sci. Rep.* 6 (2016) 20380.
- [27] B. Zhong, J. Yin, Y. Jia, L. Chen, Y. Hang, J. Yin, Laser cooling of Yb^{3+} -doped LuLiF_4 crystal, *Opt. Lett.* 39 (2014) 2747–2750.
- [28] B. Zhong, H. Luo, Y. Shi, J. Yin, Laser cooling of 5 mol. % Yb^{3+} : LuLiF_4 crystal in air, *Opt. Eng.* 56 (2016) 1–3, 3.
- [29] W. Patterson, S. Bigotta, M. Sheik-Bahae, D. Parisi, M. Tonelli, R. Epstein, Anti-Stokes luminescence cooling of Tm^{3+} doped BaY_2F_8 , *Opt. Express* 16 (2008) 1704–1710.
- [30] S. Rostami, A.R. Albrecht, A. Volpi, M. Sheik-Bahae, Observation of optical refrigeration in a holmium-doped crystal, *Photon. Res.* 7 (2019) 445–451.
- [31] A. Gragossian, J. Meng, M. Ghasemkhani, A.R. Albrecht, M. Sheik-Bahae, Astigmatic Herriott cell for optical refrigeration, *Opt. Eng.* 56 (2016), 011110.
- [32] A. Gragossian, M. Ghasemkhani, J. Meng, A. Albrecht, M. Tonelli, M. Sheik-Bahae, Optical Refrigeration Inches toward Liquid-Nitrogen Temperatures, *SPIE Newsroom*, 2017, pp. 2–4.
- [33] J. Zhang, D. Li, R. Chen, Q. Xiong, Laser cooling of a semiconductor by 40 kelvin, *Nature* 493 (2013) 504.
- [34] E.S. de Lima Filho, G. Nemova, S. Loranger, R. Kashyap, Laser-induced cooling of a Yb: YAG crystal in air at atmospheric pressure, *Opt. Express* 21 (2013) 24711–24720.
- [35] D.V. Seletskiy, M.P. Hehlen, R.I. Epstein, M. Sheik-Bahae, Cryogenic optical refrigeration, *Adv. Optic Photon* 4 (2012) 78–107.
- [36] A. Volpi, G. Cittadino, A. Di Lieto, A. Cassanho, H.P. Jenssen, M. Tonelli, Investigation of Yb-doped LiLuF_4 single crystals for optical cooling, *Opt. Eng.* 56 (2016), 011105.
- [37] S. Melgaard, D. Seletskiy, V. Polyak, Y. Asmerom, M. Sheik-Bahae, Identification of parasitic losses in Yb: YLF and prospects for optical refrigeration down to 80K, *Opt. Express* 22 (2014) 7756–7764.
- [38] G. Nemova, *Laser Cooling: Fundamental Properties and Applications*, Pan Stanford, 2016.
- [39] G. Nemova, R. Kashyap, Optical refrigeration of Yb^{3+} :YAG nanocrystals, *Proc. SPIE* 9380 (2015) 938008.
- [40] G. Cittadino, A. Volpi, A. Di Lieto, M. Tonelli, Czochralski crystal growth for laser cooling, *Opt. Eng.* 56 (2016), 011107.
- [41] A. Volpi, J. Meng, A. Gragossian, A.R. Albrecht, S. Rostami, A. Di Lieto, R. I. Epstein, M. Tonelli, M.P. Hehlen, M. Sheik-Bahae, Optical refrigeration: the role of parasitic absorption at cryogenic temperatures, *Opt. Express* 27 (2019) 29710–29718.